

Electronic Supplementary Information

Adipic Acid Directed Self-Healable Supramolecular Metallogels of Co(II) and Ni(II): Intriguing Scaffolds for Comparative Optical-Phenomenon in terms of Third Order Optical Non-Linearity

Gerald Lepcha^{a,d}, Tara Singha^{b,d}, Santanu Majumdar^a, Amit Kumar Pradhan^b, Krishna Sundar Das^c, Prasanta Kumar Datta^{b,*}, Biswajit Dey^{a,*}

^aDepartment of Chemistry, Visva-Bharati University, Santiniketan-731235, India.

^bDepartment of Physics, Indian Institute of Technology Kharagpur, Kharagpur-721302, India.

^cSchool of Chemical Sciences, Indian Association for the Cultivation of Science, Jadavpur, Kolkata, West Bengal-700032

Corresponding Author

*(B.D.) E-mail: bdeychem@gmail.com

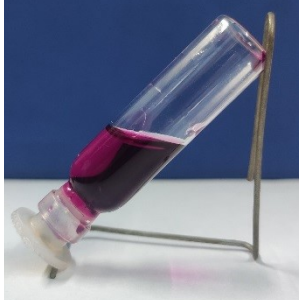

*(P.K.D.) E-mail: pkdatta@phy.iitkgp.ac.in

Author Contributions

^dAuthors are equally contributed.

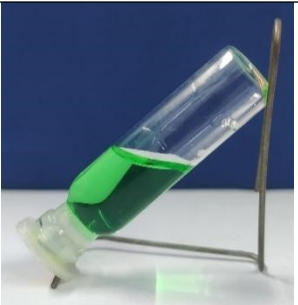

1. Experimental Section:

1.1. Table S1. Representating the influence of the counter-anion of metal salts on the gelation ability of Co-AA metallochel.^a

Entry	Metal Salt	[Metal Salt]	[Adipic acid]	Vol. ^b	Phase ^c	Picture
1	Co(NO ₃) ₂ ·6H ₂ O	1 mM	2 mM	1 mL	S	
2	CoCl ₂ ·6H ₂ O	1 mM	2 mM	1 mL	S	

^aGelation tests were performed as described in the Experimental Section. ^bTotal volume of solvent. ^cAbbreviations: S = solution.

1.2. Table S2. Representating the influence of the counter-anion of metal salts on the gelation ability of Ni-AA metallochel.^a

Entry	Metal Salt	[Metal Salt]	[Adipic acid]	Vol. ^b	Phase ^c	Picture
1	Ni(NO ₃) ₂ ·6H ₂ O	1 mM	2 mM	1 mL	S	
2	NiCl ₂ ·6H ₂ O	1 mM	2 mM	1 mL	S	

^aGelation tests were performed as described in the Experimental Section. ^bTotal volume of solvent. ^cAbbreviations: S = solution.

1.3. Testing of gelation ability of different solvents in forming stable metallogel of Co-AA and Ni-AA metallogels

Gelation ability of different solvents in forming stable metallogel of Co-AA:

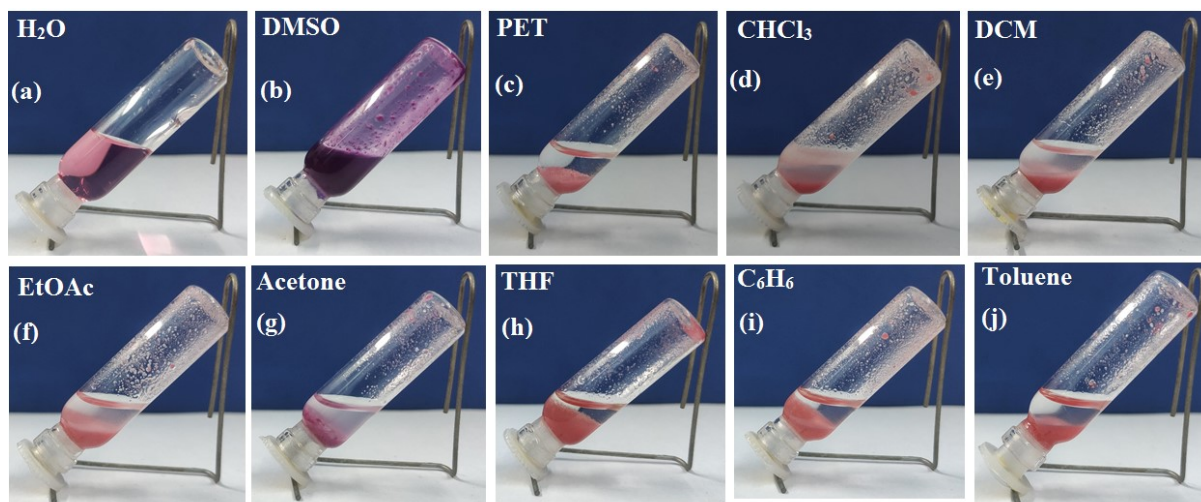


Fig. S1. Investigation of gelation ability of different solvents in forming stable metallogel of Co-AA. Here, the optimum amounts of gel-forming agents (like Co(II) acetate tetrahydrate, and adipic acid), mentioned in the synthetic part of experimental section, were maintained throughout the entire solvent dependent studies.

Gelation ability of different solvents in forming stable metallogel of Ni-AA:

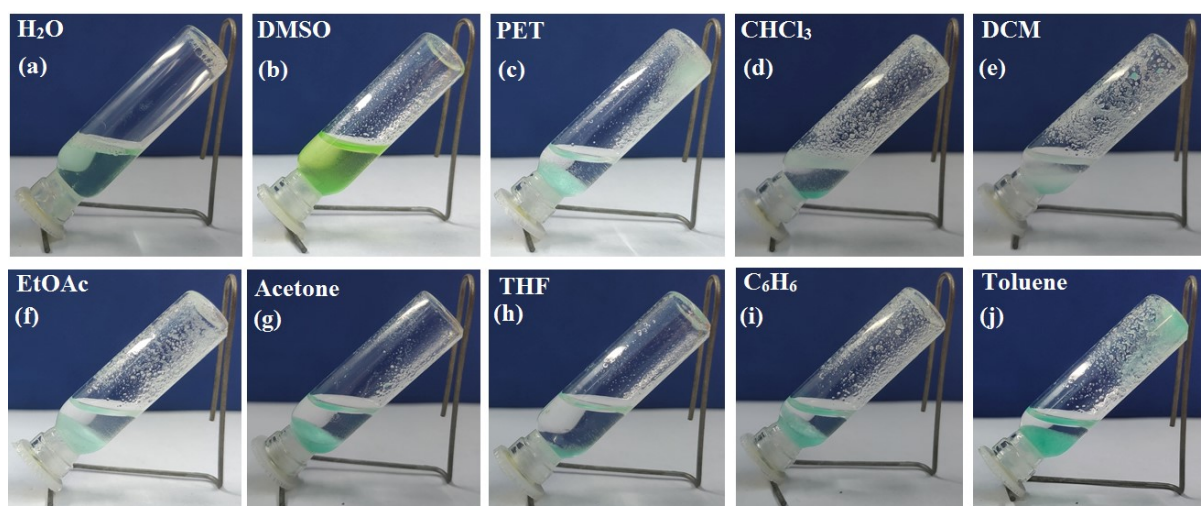
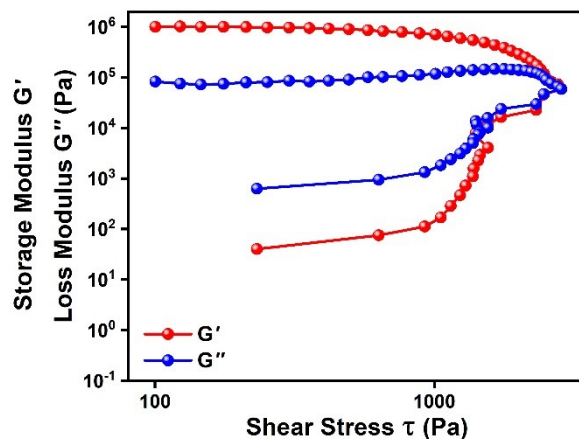
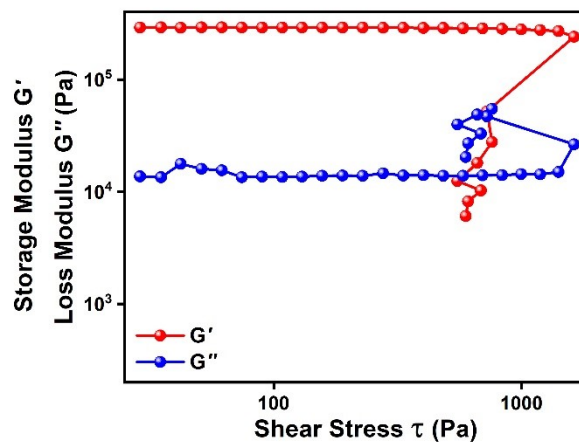


Fig. S2. Investigation of gelation ability of different solvents in forming stable metallogel of Ni-AA. The optimum amounts of gel-forming agents (like Ni(II) acetate tetrahydrate, and adipic acid), mentioned in the synthetic part of experimental section, were maintained throughout the entire solvent dependent studies.

2. Rheological Experiments:



(a)



(b)

Fig. S3 (a) Stress sweep test for Co-AA and (b) Stress sweep test for Ni-AA.

3. Z-scan Technique: In the Z-scan technique, we used 750 nm beam excitation at pulse width 100 fs and repetition rate of 1 kHz from a commercial optical parametric amplifier (TOPAS-Prime, OPA). The OPA is seeded with a Ti-sapphire (Coherent, Libra HE) regenerative amplifier laser pulse at 808 nm, 50 fs pulse width at a repetition rate of 1 kHz. A plano-convex lens of 20 cm focal length is used to focus the input laser beam. The laser stability is $\sim 2\%$. The beam waist at focus and the Rayleigh range around the focus is $\sim 50 \mu\text{m}$ and 1.05 cm respectively. The gel sample was kept inside a quartz cuvette with the effective sample length 1 mm and the cuvette was placed on a translational stage (Newport, GST-150), connected with a motion controller (Newport, ESP-150) for the scanning around the focus from $-Z$ to $+Z$ axis. The simultaneous open aperture (OA) and close aperture (CA) Z-scan measurements are performed with the linearly polarized 750 nm beam excitation at the intensity of 64 GW/cm^2 to 140 GW/cm^2 . The transmitted beam after the sample is split by a cubic beam splitter (BS_2) for the collection of simultaneous OA and CA data by photodetectors, PD_1 and PD_2 respectively. A small aperture of a diameter $\sim 1 \text{ mm}$ is placed in

front of PD₂ for CA Z-scan measurement. Two lock-in-amplifiers were used for data acquisition for a better signal-to-noise ratio. The signal-to-noise ratio of the lock-in-amplifiers in our measurement is ~25-30 dB. The translational stage and the lock-in-amplifiers are automated with Labview 2012 environment for the data collection and averaging. (Schematic diagram is shown in the main manuscript Fig: 7(a)) The sensitivity of the entire setup is reported in our previous work.¹

4. EDX spectral analyses of Co-AA and Ni-AA metallogels.

4.1. EDX spectral analysis of Co-AA metallogel:

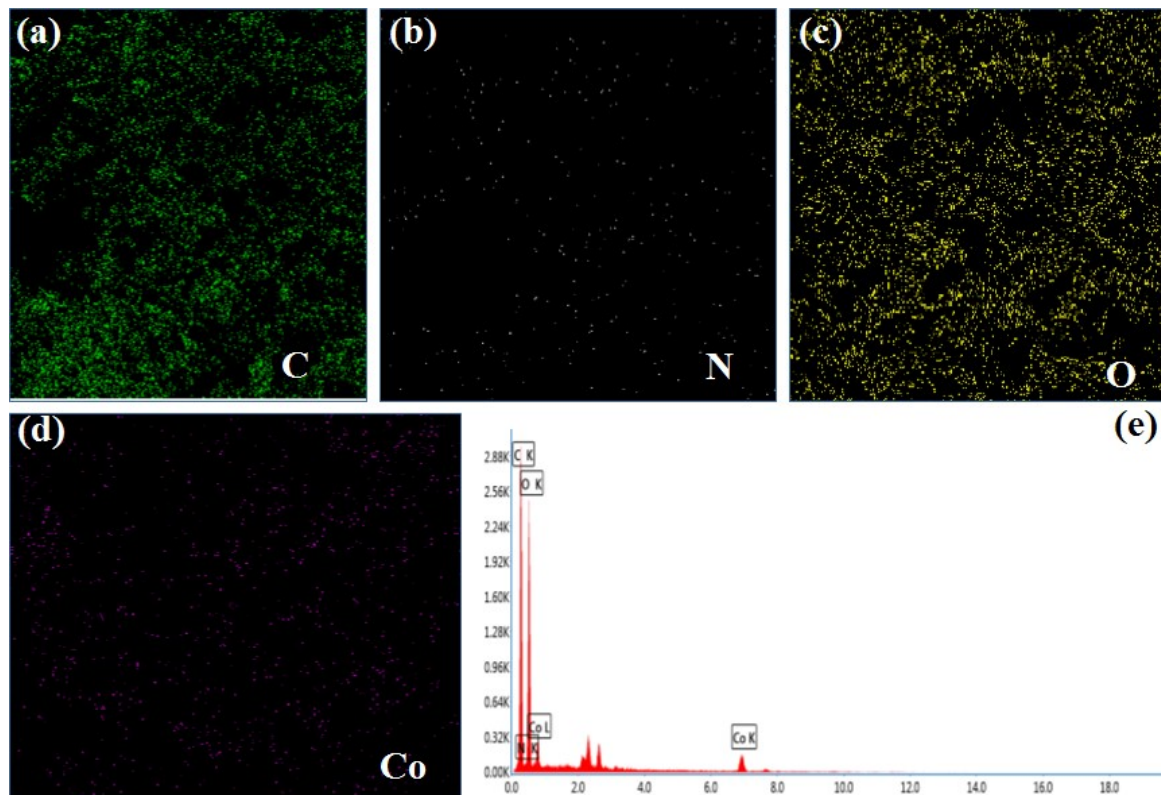


Fig.S4. (a-d) The elemental mapping of Co-AA showing the presence of C, N, O and Co elements as the constitutions of the stable metallogel, (e) EDX pattern of Co-AA metallogel.

4.2. EDX spectral analysis of Ni-AA metallo gel:

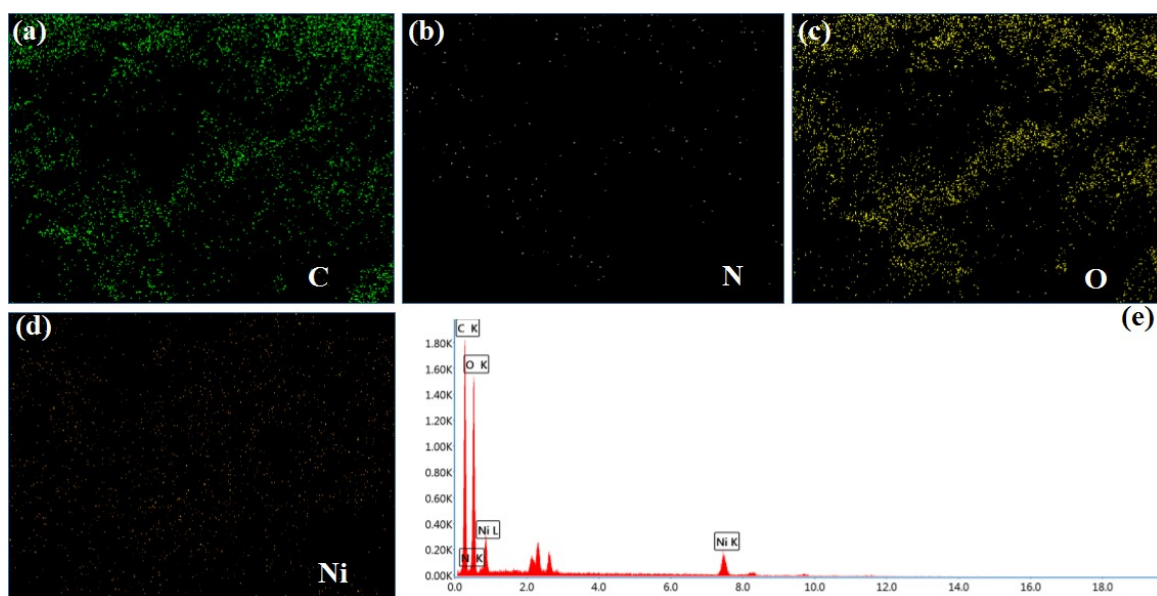


Fig. S5. (a-e) The elemental mapping of Ni-AA showing the presence of C, N, O and Ni elements as the constitutions of the stable metallo gel, (h) EDX pattern of Ni-AA metallo gel.

5. UV-Vis spectral analyses of Co-AA and Ni-AA metallo gels.

5.1. UV-Vis spectra of Co-AA metallo gel:

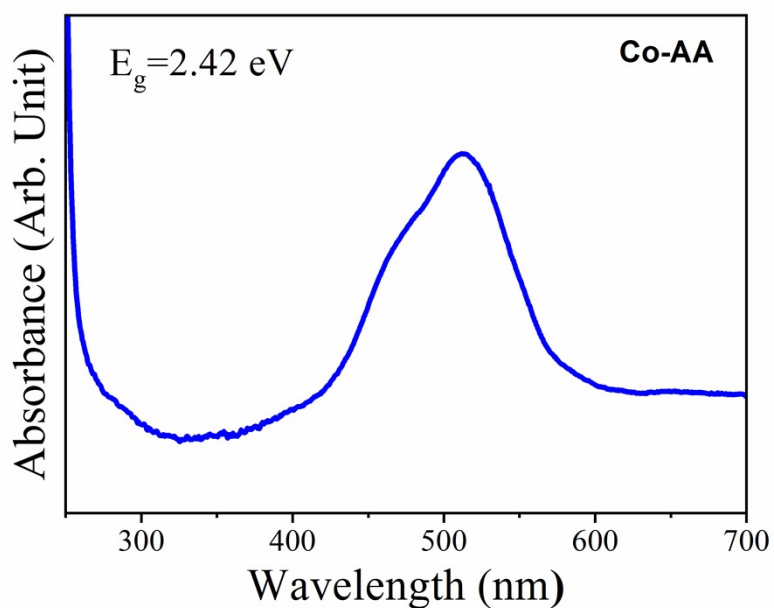


Fig. S6. UV-Vis spectra of Co-AA metallo gel.

5.2. UV-Vis spectra of Ni-AA metallogel:

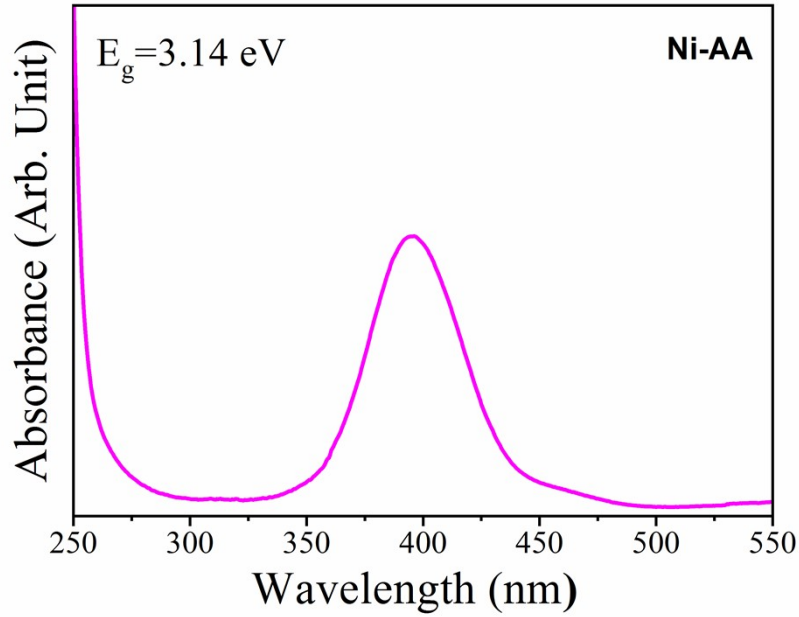


Fig. S7. UV-Vis spectra of Ni-AA metallogel.

6. Comparison table of Co-AA and Ni-AA with other materials in terms of NLO behaviour:

Table S3. Comparison of n_2^I values with other materials:

Sample	Incident Beam	n_2^I (cm ² /GW)	References
BSA-CuA	550 nm, 100 fs, 1 kHz	14.4×10^{-7}	[2]
BSA-CuCl		11.16×10^{-7}	
RGO	630 nm, 150 fs, 1 kHz	4.407×10^{-7}	[4]
ZnSe		3.595×10^{-7}	
RGO-ZnSe		4.875×10^{-7}	
CS ₂	800 nm, 110 fs, 20 Hz	3.1×10^{-6}	[5]
CdS QDs	790 nm, 130 fs, 76 MHz	1.0×10^{-6}	[6]
Co-AA	750 nm, 100 fs, 1 kHz	3.619×10^{-6}	This Work
Ni-AA		3.472×10^{-6}	

Table S4. Comparison of β values with other materials:

Sample	Incident Beam	β (cm/GW)	References
BSA-CuA	550 nm, 100 fs, 1 kHz	6.62×10^{-2}	[2]
BSA-CuCl		5.40×10^{-2}	
RGO	630 nm, 150 fs, 1 kHz	1.9×10^{-2}	[4]
ZnSe		3.3×10^{-2}	
RGO-ZnSe		1.85×10^{-1}	
CdS QDs	790 nm, 130 fs, 76 MHz	3.9×10^{-2}	[6]
C ₆₀	1064 nm, 55 fs	1.5×10^{-1}	[3]
Co-AA	750 nm, 100 fs, 1 kHz	1.503×10^{-1}	This Work
Ni-AA		1.381×10^{-1}	

References:

- (1) T. Singha, M. Karmakar, P. Kumbhakar, C. S. Tiwary and P. K. Datta, *Appl. Phys. Lett.*, 2022, **120**, 021101.
- (2) S. Majumdar, T. Singha, S. Dhibar, A. Mandal, P. K. Datta and B. Dey, *ACS Applied Electronic Materials*, 2020, **2**, 3678-3685.
- (3) R. A. Ganeev, *J. Opt. A: Pure Appl. Opt.*, 2005, **7**, 717.
- (4) A. B. Rahaman, S. Bhattacharya, A. Sarkar, T. Singha, D. Banerjee and P. K. Datta, *Journal of Applied Physics*, 2019, **126**, 233101.
- (5) S. Couris, M. Renard, O. Faucher, B. Lavorel, R. Chaux, E. Koudoumas and X. Michaut, *Chemical Physics Letters*, 2003, **369**, 318-324.
- (6) H.-M. Gong, X.-H. Wang, Y.-M. Du and Q.-Q. Wang, *J. Chem. Phys.*, 2006, **125**, 024707.